Chapter 17
Performance Improvement of RFID Systems

Abdullah Eroglu

Introduction

Radio frequency identification devices (RFIDs) have been used widely in industrial and medical applications due to the fact they bridge the real and the virtual worlds and enable information transfer at a large scale in a cost effective way. These devices use radio waves for non-contact reading and are effective in manufacturing and several other applications where bar code labels could not survive.

An RFID system includes mainly three components: *a tag or transponder* located on the object to be identified, *an interrogator* (reader) which may be a read or write/read device, and *an antenna* that emits radio signals to activate the tag and read/write data to it as shown in Fig. 17.1.

RFID tags are classified as passive, semi-active (or semi-passive), and active. Passive tag operates on its own with no source and makes use of the incoming radio waves as energy source. Active tags use the battery power for continuous operation. Semi-active tags use battery power for some functions but utilize the radio waves of the reader as an energy source for its own transmission just like passive tags. Passive tags are very popular due to the fact that they operate without need of external power source. One of the biggest challenges of passive RFID tags is their communication distance. The operating range of a RFID system is based on tag parameters such as, tag antenna gain and radar cross section, distances between readers, operating frequency, transmission power from reader to the tag, and gain of the reader antenna. As a result, tag antenna performance plays very important role in identification of the communication distance with operational frequency. Typical operational frequencies and their corresponding communication distances

A. Eroglu (✉)
Indiana University–Purdue University Fort Wayne, 2101 E. Coliseum Blvd, Fort Wayne, IN 46805, USA
e-mail: eroglua@ipfw.edu

S. C. Suh et al. (eds.), *Applied Cyber-Physical Systems*,
DOI: 10.1007/978-1-4614-7336-7_17,

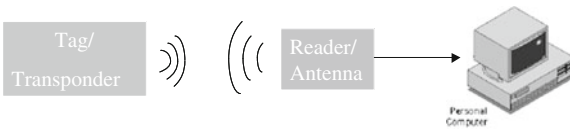

Fig. 17.1 Basic diagram of RFID system

for RFID tags are given in Table 17.1. As seen from Table 17.1, the communication distance for ultra high frequency range (UHF) is much higher than other conventional RFID frequency bands [1].

Planar type antennas such as patch antennas are widely used in RFID systems due to their several advantages including low profile, light weight, easy fabrication and conformability to mounting hosts in addition to size reduction and bandwidth enhancement. The advantages and disadvantages of patch antennas in RF systems are shown in Table 17.2. One of the cost effective solution to this challenge is the use of higher gain patch antennas with low profile. The recent advancements in EBG structures in antenna designs show that they reduce the propagating surface waves. Reduction in surface wave improve the antenna gain, directivity and bandwidth [2, 3]. In addition, the profile of the patch antenna can be further lowered when high permittivity material is used.

In this chapter, performing patch antenna design with EBG structure and high permittivity material is given for UHF RFID systems. The proposed antenna is designed and simulated with 3D electromagnetic simulator, Ansoft HFSS. Several important antenna parameters have been investigated for performance improvement and simulated results are presented. Results of this paper can be used in patch antenna design to improve its performance for applications such as biomedical and asset-tracking.

Table 17.1 RFID tags and communication distance

RFID frequency band	Frequency band	Typical communication distance (m)	Common application
125–134.2 kHz and 140–148.5 kHz	Low frequency	Up to ~½	Animal tracking access control product authentication
13.553–13.567 MHz	High frequency	Up to ~1	Smart cards shelve item tracking airline baggage maintenance
858–938 MHz, 902–928 MHz, North America	Ultra high frequency	Up to 10	Pallet tracking carton tracking electronic toll collection parking lot access
2.45 GHz/5.8 GHz	Microwave	Up to 2	Electronic toll collection airline baggage

Table 17.2 Advantages and disadvantages of patch antennas

Advantages	Disadvantages
Light weight	Narrow bandwidth
Low volume	Not the greatest gain
Low profile	Incapable of handling high power
Conformal to multiple surfaces	Extraneous radiation from junctions and feeds
Low fabrication cost	Excitation of surface waves
Feeding and matching can be fabricated simultaneously with the antenna structure	Poor efficiency from use of material with a high dielectric constant

Patch Antenna Design for RFID Systems

Conventional patch antenna shown in Fig. 17.2 is designed based on the required resonant frequency (fr), size, and bandwidth. The size and bandwidth requirements determine the dielectric constant (εr) and height (h) of the substrate. Increasing the height of the substrate increases the bandwidth, but it also increases the size of the antenna and could increase propagation of surface waves, which causes performance degradation. Meanwhile, increasing the dielectric constant decreases the size of the antenna but narrows the bandwidth. Therefore, the substrate's dielectric constant and height must be selected carefully depending on the application. Once a dielectric substrate is selected, the width (W) and length (L) of the radiating patch can be calculated. The width of the patch antenna is calculated from [4, 5]

$$W = \frac{c}{2f_r}\left(\frac{2}{\varepsilon_r + 1}\right)^{1/2} \tag{17.1}$$

The length of the patch is found using

$$L = \frac{c}{2f_r\sqrt{\varepsilon_{eff}}} - 2\Delta L \tag{17.2}$$

where

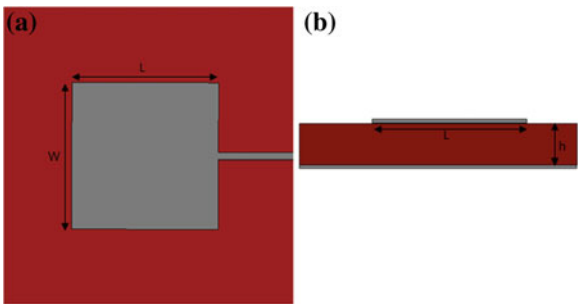

Fig. 17.2 Patch antenna: **a** *top view*, **b** *side view*

$$\Delta L = 0.412h\frac{\left(\varepsilon_{eff} + 0.3\right)\left(\frac{W}{h} + 0.264\right)}{\left(\varepsilon_{eff} - 0.258\right)\left(\frac{W}{h} + 0.8\right)} \tag{17.3}$$

and

$$\varepsilon_{eff} = \frac{\varepsilon_r + 1}{2} + \frac{\varepsilon_r - 1}{2}\left(1 + \frac{12h}{W}\right)^{-1/2} \tag{17.4}$$

Square patch antenna is designed by using Eqs. (17.2–17.4) with an Nelder–Mead optimization technique as

$$l = \frac{c}{2f_r\sqrt{\varepsilon_{eff}}} - 2(0.412h)\frac{\left(\varepsilon_{eff} + 0.3\right)\left(\frac{l}{h} + 0.264\right)}{\left(\varepsilon_{eff} - 0.258\right)\left(\frac{l}{h} + 0.8\right)} \tag{17.5}$$

To obtain a desirable return loss at the resonant frequency, a microstrip patch antenna must be matched to the transmission line feeding it. Before employing any matching technique, the resonant input impedance must be calculated. The transmission line model and cavity model can be applied to calculate the input impedance at the edge of the patch antenna. Once the edge input impedance is calculated, the different matching techniques can be employed. The transmission line model and cavity model with and without mutual effects included for various dielectric permittivity constants and dielectric substrate thicknesses have been compared through simulations with HFSS are shown in Tables 17.3 and 17.4. The transmission line model with mutual effects included was found to be the best estimate of the edge impedance for the resonant frequency of interest (915 MHz). These results were tested with probe-fed and inset-fed patch simulations using the following inset equation

$$Z_{in}(y = y_0) = Z_{in}(y = 0)\,\cos^2\left(\frac{\pi y_0}{L}\right) \tag{17.6}$$

It has been found that probe-fed antenna gives better performance than the inset-fed antenna.

Table 17.3 $Z_{in}(\Omega)$ of patch with h = 1.5 mm and f_r = 915 MHz

ε_r	Z_{in} (TL)	Z_{in} (TL−M)	Z_{in} (Cavity)	Z_{in} (Cav−M)	Sim (Z_{in})
6.5	232.4	186.4	678.0	394.1	117.6
8.9	267.0	216.0	894.0	499.2	158.5
9.8	278.9	226.5	975.0	539.0	172.8
12.88	316.1	260.1	1252.2	675.9	210.7

Table 17.4 $Z_{in}(\Omega)$ of patch with $\varepsilon_r = 9.8$ and $f_r = 915$ MHz

h (mm)	Z_{in} (T L)	Z_{in} (TL−M)	Z_{in} (Cavity)	Z_{in} (Cav−M)	Sim (Z_{in})
1.5	278.9	226.5	975.0	539.0	172.8
2.0	278.9	226.5	975.0	538.9	169.7
2.5	278.9	226.4	975.0	538.7	171.2
3.0	278.9	226.4	975.0	538.5	171.3
3.5	278.9	226.4	975.0	538.2	168.6

Patch Antenna Design with EBG Structures

EBG structure can be approximated by lumped LC elements when the operating wavelength is large compared to the periodicity as shown in Figs. 17.3 and 17.4. The small gaps between the patches generate a capacitance and the current along adjacent patches produces an inductance [6]. The impedance of a parallel resonant LC circuit is given by

$$Z = \frac{j\omega L}{1 - \omega^2 LC} \tag{17.7}$$

where the capacitance and inductance relations are obtained using

$$C = \frac{W\varepsilon_0(1 + \varepsilon_r)}{\pi}\cosh^{-1}\left(\frac{W + g}{g}\right) \tag{17.8}$$

$$L = \mu_0\mu_r h \tag{17.9}$$

The resonant frequency is then found from

$$f_r = \frac{1}{2\pi\sqrt{LC}} \tag{17.10}$$

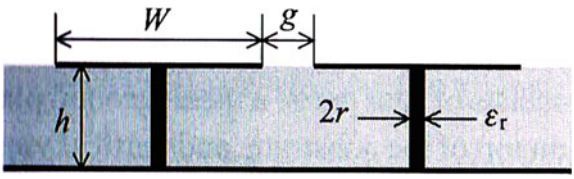

Fig. 17.3 EBG structure implementation

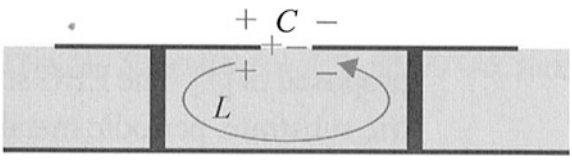

Fig. 17.4 LC equivalent model of EBG structure

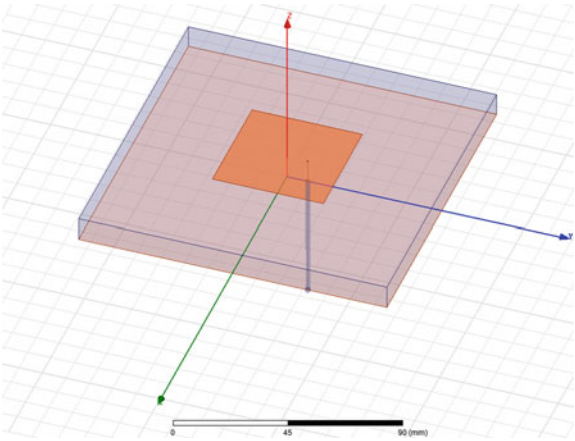

Fig. 17.5 Simulated patch antenna with EBG structure

The approximate size that is allowed for the EBG structure is obtained through the relation given below.

$$BW \propto \frac{L}{C} \tag{17.11}$$

For a frequency band gap centered at 915 MHz (UHF RFID), a patch antenna surrounded by a mushroom-like EBG structure on a typical substrate would require gaps that are small.

Patch antennas that are modeled and simulated with 3D electromagnetic simulator, HFSS, given in Fig. 17.5. Figure 17.6 show the simulated patch antenna with and without EBG structure.

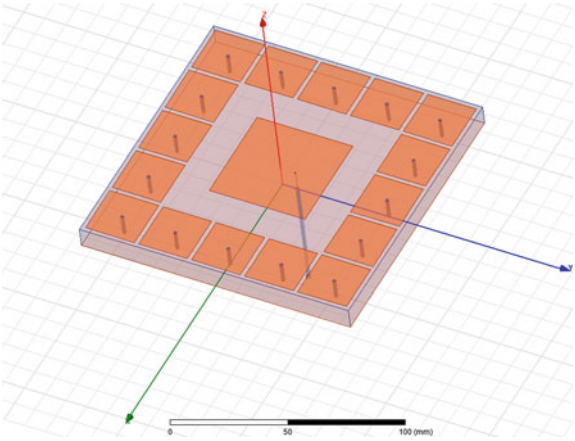

Fig. 17.6 Simulated patch antenna with EBG structure

Simulation Results

The performances of the patch antenna with and without an EBG structures are compared when high permittivity material, Alumina, with dielectric constant $\varepsilon_r = 9.8$ and thickness, h = 10 mm is used as a substrate. The performance comparison results for the patch antenna with and without EBG structures are shown in Figs. 17.5 and 17.6 have been done using 3D electromagnetic simulator HFSS. Table 17.5 outlines the physical dimensions used during the simulation of both configurations.

The gain of the patch antenna on xz and yz planes with and without EBG structures are shown in Figs. 17.7 and 17.8, respectively.

Table 17.5 Physical dimensions of the patch antennas simulated

Parameter	Patch antenna without EBG	Patch antenna with EBG	EBG structure	
Substrate			Width	23.6 mm
Height	10 mm	10 mm	Gap	2.01 mm
Dielectric constant	10.2	10.2	Radius of vias	1 mm
Length	130 mm	130 mm	Distance from patch	16.17 mm
Width	130 mm	130 mm	Number of units	16
Patch			Number of rows	1
Length	46.65 mm	46.5 mm		
Width	46.65 mm	46.5 mm		
Feed location				
y_o	14.925 mm	16.4 mm		

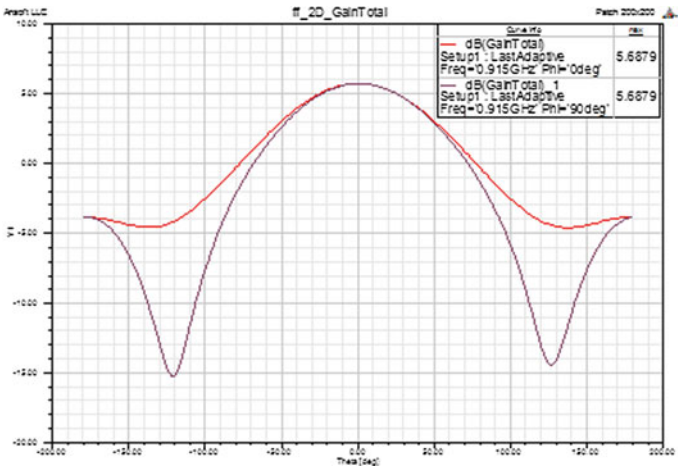

Fig. 17.7 Gain of patch antenna without EBG structures in rectangular coordinate system

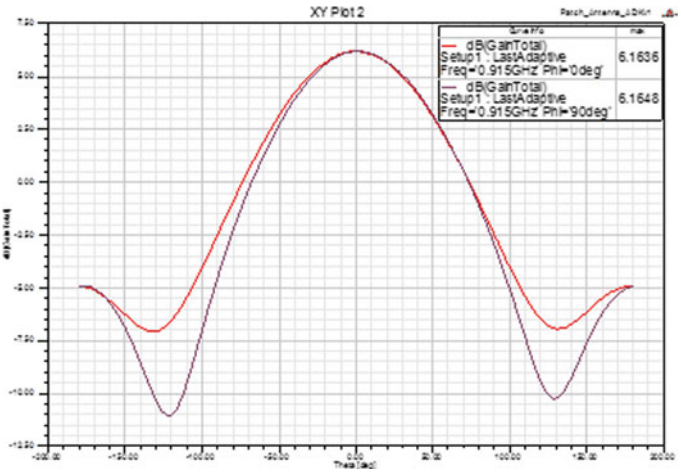

Fig. 17.8 Gain of patch antenna with EBG structures in rectangular coordinate system

As seen from the gain patterns in rectangular coordinate system, the gain improvement is around 0.5 dB when EBG structure is implemented. The strength of the minor lobe is also reduced with the use of EBG structures. This can be better demonstrated with the radiation pattern in polar coordinate system as shown in Figs. 17.9 and 17.10. Figure 17.9 shows that radiation pattern without EBG structure whereas Fig. 17.10 gives the radiation pattern of the patch antenna with EBG structure.

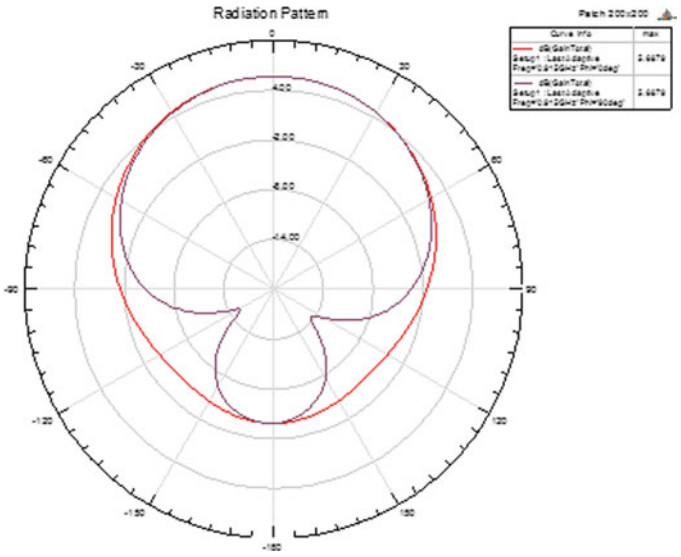

Fig. 17.9 Gain of patch antenna without EBG structures in polar coordinate system

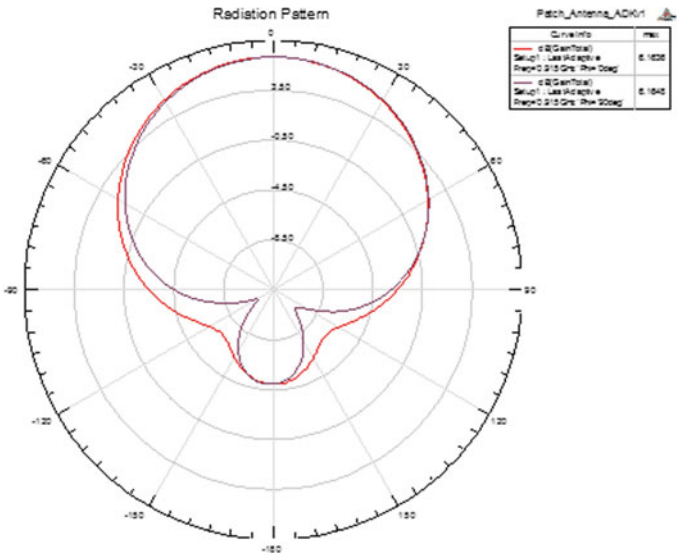

Fig. 17.10 Gain of patch antenna with EBG structures in polar coordinate system

The return losses of the patch antenna with and without EBG structure are given in Figs. 17.11 and 17.12.

The return loss of the patch antenna seems to be unaffected with the implementation of EBG structures. The bandwidth of the antenna with EBG structure is narrower. Front to back ratio of the antenna with EBG structure is around 1.5 dB higher than the same antenna without EBGs. The results showing the performance

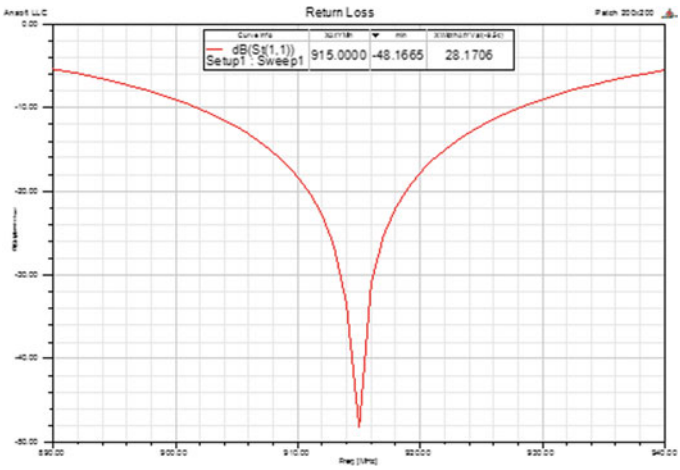

Fig. 17.11 Return loss of the patch antenna without EBG structures in polar coordinate system

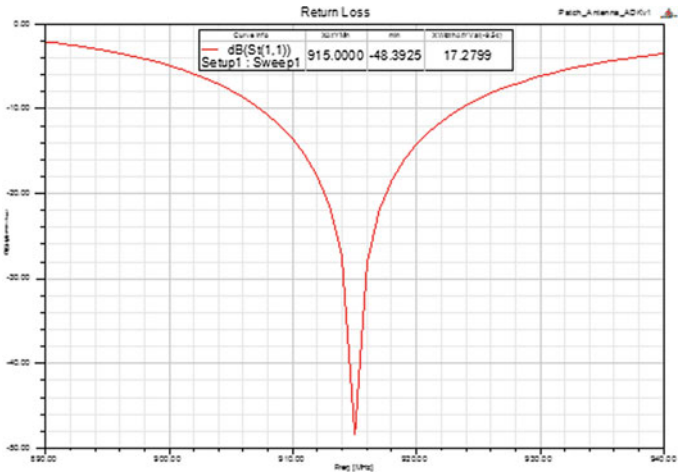

Fig. 17.12 Return loss of the patch antenna with EBG structures in polar coordinate system

of the antenna are tabulated in Table 17.6. It has been observed that the size of the ground plane also affects the radiation characteristics of the antenna. The performance of the antenna with different ground planes are also tabulated and given in Tables 17.7 and 17.8.

Table 17.6 Performance results of patch antenna with and without EBG structures

	Resonant frequency (MHz)	Return loss (dB)	Bandwidth (MHz)	Peak gain (dB)	Front-to-back (dB)
Patch without EBG	915	−48.17	28.17	5.6879	9.5497
Patch with EBG	915	−48.39	17.28	6.1648	11.0656

Table 17.7 Performance results of patch antenna without EBG structures for different ground plane sizes

Ground plane (mm × mm)	Resonant frequency (MHz)	Return loss (MHz)	Bandwidth (MHz)	Peak gain (dB)
130 × 130	915	−48.39	17.28	6.1648
200 × 200	919	−18.33	14.46	6.1917
300 × 300	918	−14.79	12.14	5.6481
500 × 500	918	−15.69	12.84	5.8219

Table 17.8 Performance results of patch antenna with EBG structures for different ground plane sizes

Ground plane (mm × mm)	Resonant frequency (MHz)	Return loss (MHz)	Bandwidth (MHz)	Peak gain (dB)
130 × 130	915	−48.39	17.28	6.1648
200 × 200	919	−18.33	14.46	6.1917
300 × 300	918	−14.79	12.14	5.6481
500 × 500	918	−15.69	12.84	5.8219

Conclusion

In this chapter, design and simulation of better performing patch antenna for UHF RFID systems with low cost is introduced using EBG structures. The simulated results for the patch antenna with and without EBG structures have been compared for antenna performance at the frequency of interest. It has been shown that gain of the antenna improve with the proposed design method. The improvement over bandwidth and return loss have also been observed with different conditions when EBG structure is implemented. The manufacturing process of the antenna is also quite straightforward since EBG structures are integrated to the overall structure. Patch antenna with EBG structure presented in this paper can be used in several applications where performance is an important parameter. This includes bio-medical and asset-tracking applications.

References

1. Omni-ID® Ultra. "*Omni-ID Passive RFID Tags: High Performance Radio Frequency Identification for RFID Asset Tracking*". Omni-ID, 2011. Web. 22 Dec. 2011.
2. T. T. Nguyen, D. Kim, S. Kim, J. Jang, "Design of a wideband mushroom-like electromagnetic bandgap structure with magneto-dielectric substrate," 6th International Conference on Information Technology and Applications, Nov. 2009, pp. 130–135.
3. Tan, M. N. Md.; Rahman, T. A.; Rahim, S. K. A.; Ali, M. T.; Jamlos, M. F., "Antenna array enhancement using mushroom-like electromagnetic band gap (EBG)," Antennas and Propagation (EuCAP), 2010 Proceedings of the Fourth European Conference on, vol., no., pp. 1–5, 12–16 April 2010.
4. Balanis, C. A., Antenna Theory: Analysis and Design (3rd edition), John Wiley & Sons, New York.
5. Fang, D. G., Antenna Theory and Microstrip Antennas, CRC Press Taylor & Francis Group, Boca Raton.
6. Yang, Fan, and Yahya Rahmat-Samii. *Electromagnetic Band Gap Structures in Antenna Engineering*. Cambridge, UK: Cambridge UP, 2009.